Fitting a triaxial ellipsoid to a geoid model

G. Panou, R. Korakitis and G. Pantazis

Department of Surveying Engineering, National Technical University of Athens, 15780 Athens, Greece

Abstract: The aim of this work is the determination of the parameters of Earth's triaxiality through a geometric fitting of a triaxial ellipsoid to a set of given points in space, as they are derived from a geoid model. Starting from a Cartesian equation of an ellipsoid in an arbitrary reference system, we develop a transformation of its coefficients into the coordinates of the ellipsoid center, of the three Euler angles and the three ellipsoid semi-axes. Furthermore, we present different mathematical models for some special and degenerate cases of the triaxial ellipsoid. We also present the required mathematical background of the theory of least-squares, under the condition of minimization of the sum of squares of geoid heights. Also, we describe a method for the determination of the foot points of the set of given space points. Then, we prepare suitable data sets and we derive results for various geoid models, which were proposed since fifty years. Among the results, we report the semi-axes of the triaxial ellipsoid of geometric fitting with four unknowns to be 6378171.92 m, 6378102.06 m and 6356752.17 m and the equatorial longitude of the major semi-axis –14.9367 degrees. Also, the parameters of Earth's triaxiality are directly estimated from the spherical harmonic coefficients of degree and order two. Finally, the results indicate that the geoid heights with respect to the triaxial ellipsoid are smaller than those with respect to the oblate spheroid and the improvement in the corresponding rms value is about 20 per cent.

Keywords: algebraic fitting, coordinates conversion, geometric fitting, least squares method, principal axes

1. Introduction

The problem of determining the parameters of Earth's triaxiality has been recognized since 1859 and various treatments by different scientists have been reported in the comprehensive list by Heiskanen (1962). Also, recent determinations of the parameters of triaxiality (semi-axes a_x, a_y and b, longitude of major semi-axis λ_0) are presented in Table 1. However, the difference between the equatorial semi-axes a_x and a_y, as determined in the satellite era, is smaller than the one previously proposed. Some of the reasons have been explained in Burša (1972).

Table 1: Parameters of Earth's triaxiality in the satellite era

Reference	a_x (m)	a_y (m)	b (m)	λ_0 (°)	$a_x - a_y$ (m)
Burša and Fialová (1993)	6378171.36 $\pm$0.30	6378101.61 $\pm$0.30	6356751.84 $\pm$0.30	–14.93 $\pm$0.05	69.75 $\pm$0.42
Burša and Šíma (1980)	6378172	6378102.7	6356752.6	–14.9	69.3
Eitschberger (1978)	6378173.435	6378103.9	6356754.4	–14.8950	69.5
Burša (1972)	6378173	6378104	6356754	–14.8	69
Burša (1970)	6378173 $\pm$10	6378105 $\pm$18	6356754 $\pm$10	–14.8 $\pm$5	68 $\pm$21

Generally, there are three methods for the determination of the parameters of triaxiality: i) the astrogeodetic, ii) the gravimetric and iii) the satellite method. The gravimetric method is given in detail by Heiskanen (1962). In this method, the parameters of triaxiality are determined using the least-squares method by minimizing the sum of squares of gravity anomalies Δg. However, in the pre-satellite era, as mentioned by Heiskanen (1962), the inability to determine the triaxiality parameters with the required accuracy is due to the lack of enough data. The satellite method is described in several papers, e.g. Burša (1970, 1971, 1972) and Burša and Šíma (1980). In this method, the requested parameters are determined using the least-squares method by minimizing the radial distance between a given geoidal point and the corresponding point on the surface of the ellipsoid. On the other hand, once some gravity field model is adopted, from the second-degree coefficients of spherical harmonics, the orientations of the principal axes and the magnitudes of the principal moments could be determined on the basis of a well-known theory (Chen and Shen, 2010).

Nowadays, we can obtain all the data required for applying any of the aforementioned methods. Indeed, there are several satellite-only or combined global gravity field models available by the International Centre for Global Earth Models (ICGEM) (http://icgem.gfz-potsdam.de/home.html). Also, according Barthelmes (2014), the satellite-only models are computed from satellite measurements alone, whereas ground and altimetry data are additionally used for the combined models. Furthermore, the spatial resolution of the satellite-only models is lower, but the accuracy is nearly uniform over the Earth.

In this work, we determine the parameters of Earth's triaxiality through a least-squares fitting of a triaxial ellipsoid to a set of 'almost equally spaced' geoid points, whose coordinates are of equal precision and are derived from a global gravity field model. The condition for the fitting is the minimization of the sum of squares of geoid heights N, known as geometric fitting (non-linear), using approximate values for the unknowns derived from an algebraic fitting (linear). Furthermore, in order to illuminate the differences between the triaxial ellipsoid and the oblate spheroid, which has been adopted in geodesy, we consider special and degenerate cases of the triaxial ellipsoid in the fitting. For this scope, we start from a Cartesian equation of an ellipsoid in an arbitrary reference system, as given in Hirvonen (1971), and we develop a transformation of the unknowns of the fitting into parameters, following the algorithm of determining an error ellipsoid from a 3×3 variance-covariance matrix (for the details see Hirvonen (1971)). Also, taking into account the improvement of the global gravity field models in the last fifty years, we also derive results for several past geoid models. Finally, we compare the results with those directly derived from the coefficients of a global gravity field model.

Theoretically, the results of geometric fitting are different from those of algebraic fitting and some of the advantages of the geometric fitting are referred in Bektas (2015). For the determination of parameters, in his work he uses the Levenberg-Marquardt algorithm for solving the non-linear least-squares problem of geometric fitting. Furthermore, for the determination of the distance between a data point and its closest point on the ellipsoid, he uses a general algorithm presented in Bektas (2014). Finally, as an application of his method he presents a numerical example using only 12 points. On the other hand, in the present work the problem of geometric fitting is solved following an iterative approach as a least-squares problem with constraints which involve additional parameters, using a very large data set. The required mathematical background of the theory of least-squares is included in Mikhail (1976) and Dermanis (2017).

2. Cartesian equation of an ellipsoid in an arbitrary reference system

The Cartesian equation of an ellipsoid, in an arbitrary reference system xyz, may be given by (Hirvonen 1971)

$$f(x, y, z) \doteq \begin{bmatrix} x - t_x & y - t_y & z - t_z \end{bmatrix} \begin{bmatrix} q_{xx} & q_{xy} & q_{xz} \\ q_{xy} & q_{yy} & q_{yz} \\ q_{xz} & q_{yz} & q_{zz} \end{bmatrix}^{-1} \begin{bmatrix} x - t_x \\ y - t_y \\ z - t_z \end{bmatrix} = 1 \tag{1}$$

where the elements of vector

$$\mathbf{t} = \begin{bmatrix} t_x \\ t_y \\ t_z \end{bmatrix} \tag{2}$$

are the coordinates of the ellipsoid center and the elements of symmetric matrix

$$\mathbf{Q} = \begin{bmatrix} q_{xx} & q_{xy} & q_{xz} \\ & q_{yy} & q_{yz} \\ \text{sym.} & & q_{zz} \end{bmatrix} \tag{3}$$

are functions of the three Euler angles θ_x, θ_y and θ_z, and the three ellipsoid semi-axes a_x, a_y and b (see subsection 2.4). Thus, the mathematical model given by Eq. (1), includes nine parameters corresponding to the spatial properties of an ellipsoid (translation, orientation, semi-axes). Also, we can consider different cases of an ellipsoid (T1 – S4), as presented in Table 2. In this table, the symbol "x" refers to a parameter that will be determined, whereas the symbol "0" indicates that the corresponding parameter is not included in the mathematical model.

Table 2: Parameters for different cases of a triaxial ellipsoid and degenerate cases

<table>
<tr><th rowspan="2">Case</th><th colspan="9">Parameters</th></tr>
<tr><th>t_x</th><th>t_y</th><th>t_z</th><th>θ_x</th><th>θ_y</th><th>θ_z</th><th>a_x</th><th>a_y</th><th>b</th></tr>
<tr><td>T1</td><td>x</td><td>x</td><td>x</td><td>x</td><td>x</td><td>x</td><td>x</td><td>x</td><td>x</td></tr>
<tr><td>T2</td><td>0</td><td>0</td><td>0</td><td>x</td><td>x</td><td>x</td><td>x</td><td>x</td><td>x</td></tr>
<tr><td>T3</td><td>x</td><td>x</td><td>x</td><td>0</td><td>0</td><td>0</td><td>x</td><td>x</td><td>x</td></tr>
<tr><td>T4</td><td>0</td><td>0</td><td>0</td><td>0</td><td>0</td><td>0</td><td>x</td><td>x</td><td>x</td></tr>
<tr><td>T5</td><td>x</td><td>x</td><td>x</td><td>0</td><td>0</td><td>x</td><td>x</td><td>x</td><td>x</td></tr>
<tr><td>T6</td><td>0</td><td>0</td><td>0</td><td>0</td><td>0</td><td>x</td><td>x</td><td>x</td><td>x</td></tr>
<tr><td>B3</td><td>x</td><td>x</td><td>x</td><td>0</td><td>0</td><td>-</td><td colspan="2">x</td><td>x</td></tr>
<tr><td>B4</td><td>0</td><td>0</td><td>0</td><td>0</td><td>0</td><td>-</td><td colspan="2">x</td><td>x</td></tr>
<tr><td>S3</td><td>x</td><td>x</td><td>x</td><td>-</td><td>-</td><td>-</td><td colspan="3">x</td></tr>
<tr><td>S4</td><td>0</td><td>0</td><td>0</td><td>-</td><td>-</td><td>-</td><td colspan="3">x</td></tr>
</table>

For each of the above mentioned cases, we present the corresponding mathematical model, as follows.

2.1. Triaxial ellipsoid and special cases

2.1.1. General case T1

Equation (1) is written equivalently as

$$[x-t_x \quad y-t_y \quad z-t_z]\begin{bmatrix} p_{xx} & p_{xy} & p_{xz} \\ p_{xy} & p_{yy} & p_{yz} \\ p_{xz} & p_{yz} & p_{zz} \end{bmatrix}\begin{bmatrix} x-t_x \\ y-t_y \\ z-t_z \end{bmatrix}=1 \tag{4}$$

or

$$\frac{p_{xx}}{d}x^2+\frac{p_{yy}}{d}y^2+\frac{p_{zz}}{d}z^2+\frac{2p_{xy}}{d}xy+\frac{2p_{xz}}{d}xz+\frac{2p_{yz}}{d}yz-\frac{2}{d}(p_{xx}t_x+p_{xy}t_y+p_{xz}t_z)x-\frac{2}{d}(p_{xy}t_x+p_{yy}t_y+p_{yz}t_z)y-\frac{2}{d}(p_{xz}t_x+p_{yz}t_y+p_{zz}t_z)z-1=0 \tag{5}$$

where

$$d=1-p_{xx}t_x^2-p_{yy}t_y^2-p_{zz}t_z^2-2p_{xy}t_xt_y-2p_{xz}t_xt_z-2p_{yz}t_yt_z \tag{6}$$

Equation (5) is of the form

$$c_{xx}x^2+c_{yy}y^2+c_{zz}z^2+c_{xy}xy+c_{xz}xz+c_{yz}yz+c_xx+c_yy+c_zz=1 \tag{7}$$

2.1.2. Special cases T2 – T6

In the following, we present the equations of special cases of a triaxial ellipsoid, which conclude in the forms T2 – T6 of Table 3.

$$\text{T2: } [x \quad y \quad z]\begin{bmatrix} q_{xx} & q_{xy} & q_{xz} \\ q_{xy} & q_{yy} & q_{yz} \\ q_{xz} & q_{yz} & q_{zz} \end{bmatrix}^{-1}\begin{bmatrix} x \\ y \\ z \end{bmatrix}=1 \tag{8}$$

$$\text{T3: } [x-t_x \quad y-t_y \quad z-t_z]\begin{bmatrix} q_{xx} & 0 & 0 \\ 0 & q_{yy} & 0 \\ 0 & 0 & q_{zz} \end{bmatrix}^{-1}\begin{bmatrix} x-t_x \\ y-t_y \\ z-t_z \end{bmatrix}=1 \tag{9}$$

$$\text{T4: } [x \quad y \quad z]\begin{bmatrix} q_{xx} & 0 & 0 \\ 0 & q_{yy} & 0 \\ 0 & 0 & q_{zz} \end{bmatrix}^{-1}\begin{bmatrix} x \\ y \\ z \end{bmatrix}=1 \tag{10}$$

$$\text{T5: } [x-t_x \quad y-t_y \quad z-t_z]\begin{bmatrix} q_{xx} & q_{xy} & 0 \\ q_{xy} & q_{yy} & 0 \\ 0 & 0 & q_{zz} \end{bmatrix}^{-1}\begin{bmatrix} x-t_x \\ y-t_y \\ z-t_z \end{bmatrix}=1 \tag{11}$$

$$\text{T6: } [x \quad y \quad z]\begin{bmatrix} q_{xx} & q_{xy} & 0 \\ q_{xy} & q_{yy} & 0 \\ 0 & 0 & q_{zz} \end{bmatrix}^{-1}\begin{bmatrix} x \\ y \\ z \end{bmatrix}=1 \tag{12}$$

2.2. Oblate spheroid without rotations

We now present the equations of special cases of an oblate spheroid without rotations, which conclude in the forms B3 and B4 of Table 3.

$$\text{B3: } \begin{bmatrix} x-t_x & y-t_y & z-t_z \end{bmatrix} \begin{bmatrix} q & 0 & 0 \\ 0 & q & 0 \\ 0 & 0 & q_{zz} \end{bmatrix}^{-1} \begin{bmatrix} x-t_x \\ y-t_y \\ z-t_z \end{bmatrix} = 1 \tag{13}$$

$$\text{B4: } \begin{bmatrix} x & y & z \end{bmatrix} \begin{bmatrix} q & 0 & 0 \\ 0 & q & 0 \\ 0 & 0 & q_{zz} \end{bmatrix}^{-1} \begin{bmatrix} x \\ y \\ z \end{bmatrix} = 1 \tag{14}$$

2.3. Sphere

Equation (1), in the degenerate case of a sphere, is written as

$$\text{S3: } \begin{bmatrix} x-t_x & y-t_y & z-t_z \end{bmatrix} \begin{bmatrix} q & 0 & 0 \\ 0 & q & 0 \\ 0 & 0 & q \end{bmatrix}^{-1} \begin{bmatrix} x-t_x \\ y-t_y \\ z-t_z \end{bmatrix} = 1 \tag{15}$$

which concludes in the form S3 of Table 3. Finally, in the special case of a sphere without translation, Eq. (1) is written as

$$\text{S4: } \begin{bmatrix} x & y & z \end{bmatrix} \begin{bmatrix} q & 0 & 0 \\ 0 & q & 0 \\ 0 & 0 & q \end{bmatrix}^{-1} \begin{bmatrix} x \\ y \\ z \end{bmatrix} = 1 \tag{16}$$

which concludes in the form S4 of Table 3.

Table 3: Mathematical models for different cases of a triaxial ellipsoid and degenerate cases

Case	m_0	Mathematical model
T1	9	$c_{xx}x^2 + c_{yy}y^2 + c_{zz}z^2 + c_{xy}xy + c_{xz}xz + c_{yz}yz + c_x x + c_y y + c_z z = 1$
T2	6	$c_{xx}x^2 + c_{yy}y^2 + c_{zz}z^2 + c_{xy}xy + c_{xz}xz + c_{yz}yz = 1$
T3	6	$c_{xx}x^2 + c_{yy}y^2 + c_{zz}z^2 + c_x x + c_y y + c_z z = 1$
T4	3	$c_{xx}x^2 + c_{yy}y^2 + c_{zz}z^2 = 1$
T5	7	$c_{xx}x^2 + c_{yy}y^2 + c_{zz}z^2 + c_{xy}xy + c_x x + c_y y + c_z z = 1$
T6	4	$c_{xx}x^2 + c_{yy}y^2 + c_{zz}z^2 + c_{xy}xy = 1$
B3	5	$c(x^2 + y^2) + c_{zz}z^2 + c_x x + c_y y + c_z z = 1$
B4	2	$c(x^2 + y^2) + c_{zz}z^2 = 1$
S3	4	$c(x^2 + y^2 + z^2) + c_x x + c_y y + c_z z = 1$
S4	1	$c(x^2 + y^2 + z^2) = 1$

The determination of m_0 elements of vector $\mathbf{c}$ (i.e. of the unknowns) can be accomplished by either an algebraic or a geometric fit to a given set of k points, where $k > m_0$, as presented in Sections 3 and 5, respectively.

2.4. Transformation of vector c into vector t and matrix Q (or into parameters)

In this subsection, we present the transformation of the elements of vector **c** into vector **t** and the matrix **Q** for the general case of a triaxial ellipsoid (Case T1). From Eqs. (5) to (7), we have

$$\mathbf{t} = \begin{bmatrix} t_x \\ t_y \\ t_z \end{bmatrix} = -\begin{bmatrix} 2c_{xx} & c_{xy} & c_{xz} \\ c_{xy} & 2c_{yy} & c_{yz} \\ c_{xz} & c_{yz} & 2c_{zz} \end{bmatrix}^{-1} \begin{bmatrix} c_x \\ c_y \\ c_z \end{bmatrix} \tag{17}$$

and

$$\mathbf{Q} = D \begin{bmatrix} c_{xx} & c_{xy}/2 & c_{xz}/2 \\ c_{xy}/2 & c_{yy} & c_{yz}/2 \\ c_{xy}/2 & c_{yz}/2 & c_{zz} \end{bmatrix}^{-1} \tag{18}$$

where

$$D = 1 + c_{xx}t_x^2 + c_{yy}t_y^2 + c_{zz}t_z^2 + c_{xy}t_xt_y + c_{xz}t_xt_z + c_{yz}t_yt_z \tag{19}$$

Once the matrix **Q** is determined, we apply the Singular Value Decomposition (SVD is a well-known procedure, included in most mathematical software packages) and we obtain

$$\mathbf{Q} = \mathbf{R}^{\mathrm{T}}\boldsymbol{\Lambda}\mathbf{R} \tag{20}$$

which gives directly the orthogonal rotation matrix

$$\mathbf{R} = \begin{bmatrix} r_{11} & r_{12} & r_{13} \\ r_{21} & r_{22} & r_{23} \\ r_{31} & r_{32} & r_{33} \end{bmatrix} = \begin{bmatrix} \mathrm{c}_y\mathrm{c}_z & \mathrm{c}_x\mathrm{s}_z + \mathrm{s}_x\mathrm{s}_y\mathrm{c}_z & \mathrm{s}_x\mathrm{s}_z - \mathrm{c}_x\mathrm{s}_y\mathrm{c}_z \\ -\mathrm{c}_y\mathrm{s}_z & \mathrm{c}_x\mathrm{c}_z - \mathrm{s}_x\mathrm{s}_y\mathrm{s}_z & \mathrm{s}_x\mathrm{c}_z + \mathrm{c}_x\mathrm{s}_y\mathrm{s}_z \\ \mathrm{s}_y & -\mathrm{s}_x\mathrm{c}_y & \mathrm{c}_x\mathrm{c}_y \end{bmatrix} \tag{21}$$

where, for instance, $\mathrm{c}_x\mathrm{s}_z = \cos\theta_x \sin\theta_z$, i.e. the Euler angles

$$\theta_x = \operatorname{atan}\left(\frac{-r_{32}}{r_{33}}\right), \quad \theta_y = \operatorname{atan}\left(\frac{r_{31}}{\sqrt{r_{11}^2 + r_{21}^2}}\right), \quad \theta_z = \operatorname{atan}\left(\frac{-r_{21}}{r_{11}}\right) \tag{22}$$

and the diagonal matrix

$$\boldsymbol{\Lambda} = \begin{bmatrix} \lambda_1 & 0 & 0 \\ 0 & \lambda_2 & 0 \\ 0 & 0 & \lambda_3 \end{bmatrix} \tag{23}$$

i.e. the semi-axes of the ellipsoid

$$a_x = \sqrt{\lambda_1},\ \ a_y = \sqrt{\lambda_2},\ \ b = \sqrt{\lambda_3} \tag{24}$$

We note that the rows of matrix **R** are the components of the unit vectors that correspond to the semi-axes of the ellipsoid. Also, from the 2×2 submatrices of matrix **Q** we obtain ellipses on the three planes containing the axes of the xyz system, thus we can easily investigate the proper sign of the Euler angles. Finally, we can apply the appropriate parts of the transformation in all special and degenerate cases.

3. Algebraic (linear) fitting

In this section, we present the process of algebraic fitting in the general case of a triaxial ellipsoid (T1), in order to obtain the best estimates of elements of vector **c**. We use the method of least squares, assuming that the Cartesian coordinates of the given points (X_i, Y_i, Z_i) are of equal precision, uncorrelated and are identical with the coordinates of foot points (x_i, y_i, z_i). Thus, we can write the linear Eq. (7) in the form

$$c_{xx}x_i^2 + c_{yy}y_i^2 + c_{zz}z_i^2 + c_{xy}x_iy_i + c_{xz}x_iz_i + c_{yz}y_iz_i + c_xx_i + c_yy_i + c_zz_i = 1 + \upsilon_i,\ \ i = 1, \dots, k \tag{25}$$

which can be represented in matrix form as

$$\mathbf{Dc} = \mathbf{i} + \boldsymbol{\upsilon} \tag{26}$$

where

$$\mathbf{D} = \begin{bmatrix} x_1^2 & y_1^2 & \cdots & z_1 \\ \vdots & \vdots & \ddots & \vdots \\ x_k^2 & y_k^2 & \cdots & z_k \end{bmatrix} \tag{27}$$

is a $k \times m_0$ matrix containing the coefficients of the elements of vector **c** (design matrix), **i** is a $k \times 1$ vector with all elements equal to 1 and $\boldsymbol{\upsilon}$ is a $k \times 1$ vector of residuals. Then, the solution vector is given by

$$\mathbf{c} = \left(\mathbf{D}^{\mathrm{T}}\mathbf{D}\right)^{-1}\mathbf{D}^{\mathrm{T}}\mathbf{i} \tag{28}$$

Subsequently, we can compute the vector **t**, the rotation matrix **R**, i.e. the Euler angles and the matrix $\boldsymbol{\Lambda}$, i.e. the semi-axes of the ellipsoid, following the descriptions in subsection 2.4. Finally, all the special and degenerate cases can be easily obtained by suitable modifications of the matrix **D**.

4. Determination of the foot points and statistical indexes

In order to apply the geometric (non-linear) fitting, at first we compute the projections (x_i, y_i, z_i) of the given points (X_i, Y_i, Z_i) on the surface of the ellipsoid with the estimated parameters, in the same reference system xyz. To do this, we convert the coordinates of the given points (X_i, Y_i, Z_i)

to the ellipsoid aligned reference system uvw, using the known translation vector $\mathbf{t}$ (Eq. (2)) and the rotation matrix $\mathbf{R}$ (Eq. (21)), as follows:

$$\begin{bmatrix} U_i \\ V_i \\ W_i \end{bmatrix} = \begin{bmatrix} r_{11} & r_{12} & r_{13} \\ r_{21} & r_{22} & r_{23} \\ r_{31} & r_{32} & r_{33} \end{bmatrix} \begin{bmatrix} X_i - t_x \\ Y_i - t_y \\ Z_i - t_z \end{bmatrix}, \quad i = 1, \dots, k \tag{29}$$

Now, for every point (U_i, V_i, W_i), the desired projection (u_i, v_i, w_i) can be computed by any of the relevant methods of conversion of Cartesian to geodetic coordinates (e.g. Ligas (2012), Panou and Korakitis (2019)), using the known semi-axes a_x, a_y and b. Finally, the foot points (u_i, v_i, w_i) are expressed in the reference system xyz, as follows:

$$\begin{bmatrix} x_i \\ y_i \\ z_i \end{bmatrix} = \begin{bmatrix} t_x \\ t_y \\ t_z \end{bmatrix} + \begin{bmatrix} r_{11} & r_{21} & r_{31} \\ r_{12} & r_{22} & r_{32} \\ r_{13} & r_{23} & r_{33} \end{bmatrix} \begin{bmatrix} u_i \\ v_i \\ w_i \end{bmatrix}, \quad i = 1, \dots, k \tag{30}$$

since $\mathbf{R}^{-1} = \mathbf{R}^{\mathrm{T}}$. From the foot points, we can compute the geoid heights by

$$N_i = \sqrt{(U_i - u_i)^2 + (V_i - v_i)^2 + (W_i - w_i)^2} = \sqrt{(X_i - x_i)^2 + (Y_i - y_i)^2 + (Z_i - z_i)^2}, \quad i = 1, \dots, k \tag{31}$$

Also, we can compute the statistical indexes $min(N)$, $max(N)$,

$$mean(N) = \frac{1}{k} \sum_{i=1}^{k} N_i \tag{32}$$

and the root mean square (rms)

$$rms(N) = \sqrt{\frac{1}{k} \sum_{i=1}^{k} N_i^2} \tag{33}$$

5. Geometric (non-linear) fitting

In a similar manner, in this section we present the process of geometric fitting in the general case of a triaxial ellipsoid (T1). For the given points (X_i, Y_i, Z_i) (assuming unweighted and uncorrelated data) and their foot points (x_i, y_i, z_i), $i = 1, \dots, k$, the 'observation' equations are

$$x_i = X_i + v_{X_i} \tag{34}$$

$$y_i = Y_i + v_{Y_i} \tag{35}$$

$$z_i = Z_i + v_{Z_i} \tag{36}$$

while the constraints are

$$g_i \doteq c_{xx} x_i^2 + c_{yy} y_i^2 + c_{zz} z_i^2 + c_{xy} x_i y_i + c_{xz} x_i z_i + c_{yz} y_i z_i + c_x x_i + c_y y_i + c_z z_i = 1 \tag{37}$$

In the above formulation, we have $n = 3k$ measurements (observations), for the determination of $3k + m_0$ unknowns ($3k$ for (x_i, y_i, z_i) and m_0 for $\mathbf{c}$) subject to k constraints. Thus, the actual number of unknowns is $m = (3k + m_0) - k = 2k + m_0$. Since the constraints are non-linear equations, we need to linearize all equations using approximate values $\mathbf{r}^0 = [x_1^0 \quad y_1^0 \quad z_1^0 \quad \cdots \quad x_k^0 \quad y_k^0 \quad z_k^0]^{\mathrm{T}}$ and $\mathbf{c}^0$ for the unknowns $\hat{\mathbf{r}} = \mathbf{r}^0 + \boldsymbol{\delta}\mathbf{r}$ and $\hat{\mathbf{c}} = \mathbf{c}^0 + \boldsymbol{\delta}\mathbf{c}$. The approximate values $\left(x_i^0, y_i^0, z_i^0\right)$ may be computed as foot points on the ellipsoid with parameters $\mathbf{c}^0$ resulting from the algebraic fitting (Section 3), using the approach proposed in Section 4. Thus, the linear approximation of Eqs. (34) to (36) and (37) can be represented in matrix form as

$$\boldsymbol{\delta}\mathbf{r} = \boldsymbol{\delta}\mathbf{l} + \boldsymbol{\upsilon} \tag{38}$$

and

$$\mathbf{C}\boldsymbol{\delta}\mathbf{r} + \mathbf{D}\boldsymbol{\delta}\mathbf{c} = \mathbf{w} \tag{39}$$

where

$$\mathbf{C} = \mathbf{J}_{\mathbf{gr}}^0 = \begin{bmatrix} \left.\frac{\partial g_1}{\partial x_1}\right|^0 & \left.\frac{\partial g_1}{\partial y_1}\right|^0 & \left.\frac{\partial g_1}{\partial z_1}\right|^0 & 0 & 0 & 0 & \cdots & 0 & 0 & 0 \\ 0 & 0 & 0 & \left.\frac{\partial g_2}{\partial x_2}\right|^0 & \left.\frac{\partial g_2}{\partial y_2}\right|^0 & \left.\frac{\partial g_2}{\partial z_2}\right|^0 & \cdots & 0 & 0 & 0 \\ \vdots & \vdots & \vdots & \vdots & \vdots & \vdots & \ddots & \vdots & \vdots & \vdots \\ 0 & 0 & 0 & 0 & 0 & 0 & \cdots & \left.\frac{\partial g_k}{\partial x_k}\right|^0 & \left.\frac{\partial g_k}{\partial y_k}\right|^0 & \left.\frac{\partial g_k}{\partial z_k}\right|^0 \end{bmatrix} \tag{40}$$

is a $k \times n$ matrix containing the partial derivatives (Jacobian matrix)

$$\frac{\partial g_i}{\partial x_i} = 2c_{xx}x_i + c_{xy}y_i + c_{xz}z_i + c_x \tag{41}$$

$$\frac{\partial g_i}{\partial y_i} = 2c_{yy}y_i + c_{xy}x_i + c_{yz}z_i + c_y \tag{42}$$

$$\frac{\partial g_i}{\partial z_i} = 2c_{zz}z_i + c_{xz}x_i + c_{yz}y_i + c_z \tag{43}$$

$\mathbf{D} = \mathbf{J}_{\mathbf{gc}}^0$ is a $k \times m_0$ matrix, as in linear fitting (Eq. (27)) for the approximate values of the foot points $\left(x_i^0, y_i^0, z_i^0\right)$,

$$\boldsymbol{\delta}\mathbf{l} = \begin{bmatrix} X_1 - x_1^0 \\ Y_1 - y_1^0 \\ Z_1 - z_1^0 \\ \vdots \\ X_k - x_k^0 \\ Y_k - y_k^0 \\ Z_k - z_k^0 \end{bmatrix} \tag{44}$$

is a $n \times 1$ vector, $\boldsymbol{\upsilon}$ is a $n \times 1$ vector of residuals and

$$\mathbf{w} = \begin{bmatrix} 1 - g_1(x_1^0, y_1^0, z_1^0, \mathbf{c}^0) \\ \vdots \\ 1 - g_k(x_k^0, y_k^0, z_k^0, \mathbf{c}^0) \end{bmatrix} \tag{45}$$

is a $k \times 1$ vector. The above problem consists a least squares problem with constraints which involve additional parameters (see e.g. Mikhail (1976)). Then, the corrections $\boldsymbol{\delta}\mathbf{c}$ and $\boldsymbol{\delta}\mathbf{r}$ to the approximate values, in our specific case where $\mathbf{A} = \mathbf{I}$ and the weight matrix $\mathbf{P} = \mathbf{I}$, are

$$\boldsymbol{\delta}\mathbf{c} = \mathbf{L}^{-1}\mathbf{D}^{\mathrm{T}}\mathbf{K}^{-1}(\mathbf{w} - \mathbf{C}\boldsymbol{\delta}\mathbf{l}) \tag{46}$$

and

$$\boldsymbol{\delta}\mathbf{r} = \boldsymbol{\delta}\mathbf{l} + \mathbf{C}^{\mathrm{T}}\mathbf{K}^{-1}(\mathbf{w} - \mathbf{C}\boldsymbol{\delta}\mathbf{l} - \mathbf{D}\boldsymbol{\delta}\mathbf{c}) \tag{47}$$

where

$$\mathbf{K} = \mathbf{C}\mathbf{C}^{\mathrm{T}} \tag{48}$$

is a diagonal matrix and

$$\mathbf{L} = \mathbf{D}^{\mathrm{T}}\mathbf{K}^{-1}\mathbf{D} \tag{49}$$

Furthermore, the a-posteriori variance factor $\hat{\sigma}_0^2$ is computed by

$$\hat{\sigma}_0^2 = \frac{\boldsymbol{\upsilon}^{\mathrm{T}}\boldsymbol{\upsilon}}{n-m} = \frac{(\boldsymbol{\delta}\mathbf{r}-\boldsymbol{\delta}\mathbf{l})^{\mathrm{T}}(\boldsymbol{\delta}\mathbf{r}-\boldsymbol{\delta}\mathbf{l})}{k-m_0} \tag{50}$$

where $n - m$ represents the degrees of freedom, while the vector of residuals $\boldsymbol{\upsilon}$ is computed from Eq. (38). Finally, the a-posteriori variance-covariance matrix of the vector $\hat{\mathbf{c}}$ is given by

$$\hat{\mathbf{V}}_{\hat{\mathbf{c}}} = \hat{\sigma}_0^2\mathbf{L}^{-1} \tag{51}$$

Finally, we can compute the coordinates of the ellipsoid center, the Euler angles and the semi-axes of the ellipsoid, according to the description in subsection 2.4.

Theoretically, the solution process is iterative until the corrections in the approximate values become negligible. It is worth emphasizing that the minimization problem solved in the geometric approach satisfies the equation $\sum_{i=1}^{k} N_i^2 = \min$. This can be checked with repetition of the process described in Section 4 and the computation of the new statistic indexes $min(\hat{N})$, $max(\hat{N})$, $mean(\hat{N})$ and $rms(\hat{N})$.

5.1. Uncertainty estimates

From Eq. (17) and using the assumption that $c_{xy} \cong c_{xz} \cong c_{yz} \approx 0$, the coordinates of the ellipsoid's center are computed simply as

$$t_x = -\frac{1}{2}\frac{c_x}{c_{xx}} \tag{52}$$

$$t_y = -\frac{1}{2}\frac{c_y}{c_{yy}} \tag{53}$$

$$t_z = -\frac{1}{2}\frac{c_z}{c_{zz}} \tag{54}$$

Thus, the uncertainties σ are computed by applying the error propagation law

$$\sigma_{t_x} = \pm\frac{1}{2}\sqrt{\left(\frac{c_x}{c_{xx}^2}\right)^2 \sigma_{c_{xx}}^2 + \left(-\frac{1}{c_{xx}}\right)^2 \sigma_{c_x}^2} \tag{55}$$

$$\sigma_{t_y} = \pm\frac{1}{2}\sqrt{\left(\frac{c_y}{c_{yy}^2}\right)^2 \sigma_{c_{yy}}^2 + \left(-\frac{1}{c_{yy}}\right)^2 \sigma_{c_y}^2} \tag{56}$$

$$\sigma_{t_z} = \pm\frac{1}{2}\sqrt{\left(\frac{c_z}{c_{zz}^2}\right)^2 \sigma_{c_{zz}}^2 + \left(-\frac{1}{c_{zz}}\right)^2 \sigma_{c_z}^2} \tag{57}$$

where σ_c are the uncertainties of the elements of vector **c**, as computed from the fitting. Also, the uncertainty of the ellipsoid semi-axes can be approximated by

$$\sigma_{a_x} \cong \sigma_{a_y} \cong \sigma_b \approx \frac{\hat{\sigma}_0}{\sqrt{k}} \tag{58}$$

where k is the number of points of fitting. Finally, the uncertainty of the orientation of the ellipsoid, can be approximated by

$$\sigma_{\theta_x} \cong \sigma_{\theta_y} \approx \frac{\hat{\sigma}_0}{b\sqrt{k}} \tag{59}$$

and

$$\sigma_{\theta_z} \approx \frac{\hat{\sigma}_0}{a_y\sqrt{k}} \tag{60}$$

6. Data and numerical results

6.1. Data

The methodology described above was applied to an extensive set of points in space, corresponding to points of the geoid, at particular values of geodetic coordinates φ and λ, using values of the geoid undulation N provided by the ICGEM service for several gravity field models.

The grid of points used was roughly equidistant, with a spatial resolution determined by the maximum degree of the gravity field model. For example, the model GOCO06s has a maximum degree 300, so the equivalent resolution (0.6 degrees) corresponds to a spatial resolution (half wavelength) of about 67 km at the equator.

The geodetic coordinates of the grid were determined by setting up a number of points along circles of equal latitude, separated by the given resolution. The angular separation along these circles (longitude difference) was increased at each latitude step (kept constant at the value of the angular resolution of the model) so that the spatial distance of points along each latitude circle remained roughly constant. In this way, the resulting grid has a uniform surface density of points, in contrast to a regular grid of (φ, λ) values, which is denser towards the poles (dataset D1.1 in Table 4).

The geodetic coordinates $(\varphi_i, \lambda_i, N_i)$ of a point on the geoid are related to the corresponding Cartesian coordinates (X_i, Y_i, Z_i) by the well-known expressions

$$X_i = (N_c + N_i)\cos\varphi_i\cos\lambda_i \tag{61}$$

$$Y_i = (N_c + N_i)\cos\varphi_i\sin\lambda_i \tag{62}$$

$$Z_i = \left[\left(\frac{b}{a}\right)^2 N_c + N_i\right]\sin\varphi_i \tag{63}$$

where

$$N_c = \frac{a^2}{\sqrt{a^2\cos^2\varphi_i + b^2\sin^2\varphi_i}} \tag{64}$$

is the radius of curvature in the prime vertical normal section, with a and b the major and minor semiaxis of the oblate spheroid, respectively. In the case of WGS 84 we have: $a = 6378137.0$ and $f = 1/298.257223563$ ($b = a(1-f)$) (NIMA (2000)).

Five different gravity field models were used in the ellipsoid fitting, which represent different stages of our knowledge about the gravity field in the last fifty years, as follows:

- GOGO06s, described by Kvas et al. (2019)
- EGM2008, described by Pavlis et al. (2012)
- EGM96, described by Lemoine et al. (1998)
- OSU86f, described by Rapp and Cruz (1986)
- GEM8, described by Wagner et al. (1977)
- SE1, described by Lundquist and Veis (1966)

For more details regarding the evaluation of these models, please visit http://icgem.gfz-potsdam.de/home.html.

Table 4 summarizes the relevant data for each data set, as well as some important statistical properties of each model for the particular grid of points used.

Table 4: Characteristics of the data sets used

Dataset	Geoid model	Spatial resolution (km)	Number of points	Statistics			
				$mean(N)$ (m)	$min(N)$ (m)	$max(N)$ (m)	$rms(N)$ (m)
D1.1	GOGO06s ($\pm$0.15 m)	Variable	179402	-0.90	-106.27	84.93	29.28
D1.2		67	114446	-0.05	-106.33	85.31	30.59
D2.1	EGM2008 ($\pm$0.15 m)	56	164836	-0.06	-106.43	85.92	30.59
D2.2		67	114446	-0.06	-106.26	85.31	30.60
D2.3		111	41164	-0.06	-105.93	85.92	30.60
D2.4		1334	286	-0.13	-94.59	72.39	30.59
D3	EGM96 ($\pm$0.50 m)	56	164836	-0.05	-106.48	85.44	30.59
D4	OSU86f ($\pm$1.5 m)	56	164836	0.02	-107.21	82.20	30.53
D5	GEM8 ($\pm$3 m)	801	769	0.13	-102.14	74.42	30.58
D6	SE1 ($\pm$10 m)	1334	286	44.12	-34.74	101.20	51.83

We should note that the great values of the *mean* and *rms* quantities for the SE1 model are due to the fact that the oblate spheroid used at the time was different from the WGS 84. In any case, the particulars of the reference spheroid do not affect the preparation of the data sets. Therefore, we decided to use WGS 84 as a common reference for all models, since it is also more realistic than the older reference surfaces.

In all numerical computations that are presented in the following sections, we used a personal computer running a 64-bit Linux Debian operating system, with an Intel Core i5-2430M CPU (clocked at 2.4 GHz) and 6 GB RAM. All algorithms were coded in C++ and compiled by the open-source GNU GCC compiler (Level 2 optimization). The computations for the fittings (both algebraic and geometric) were performed at quad precision (33 digits accuracy) using the open source "libquadmath", the GCC Quad Precision Math Library. The computations for the foot points, following the method presented in Panou and Korakitis (2019), were performed using the "long double" data type, which provides an accuracy of 18 digits.

6.2. Results and statistics for the geoid model GOCO06s

Using the data sets derived from the GOCO06s geoid model (a satellite-only model) we obtained the results for the ellipsoid parameters and the relevant statistics for all cases as presented in Tables 5 and 6, respectively.

Table 5: Resulting values of the parameters of fitting for the geoid model GOGO06s

Dataset	Fitting – Case	Parameters								
		t_x (m)	t_y (m)	t_z (m)	θ_x (°)	θ_y (°)	θ_z (°)	a_x (m)	a_y (m)	b (m)
D1.1	A - T1	5.43	0.55	6.93	-0.0048	-0.0056	-13.9666	6378173.07	6378102.94	6356749.49
D1.2	A - T1	-0.08	-0.05	-0.04	-0.000020	-0.000056	-14.9283215	6378171.918	6378102.064	6356752.169

	G - T1	-0.11 ±0.13	-0.05 ±0.13	-0.06 ±0.13	0.0000043 ±0.0000007	-0.000083 ±0.0000007	-14.9366733 ±0.0000007	6378171.915 ±0.07	6378102.061 ±0.07	6356752.175 ±0.07
	G - T2	0	0	0	0.0000043 ±0.0000007	-0.000083 ±0.0000007	-14.9366732 ±0.0000007	6378171.92 ±0.07	6378102.06 ±0.07	6356752.17 ±0.07
	G - T3	-0.11 ±0.13	-0.05 ±0.13	-0.06 ±0.13	0	0	0	6378167.27 ±0.08	6378106.70 ±0.08	6356752.17 ±0.08
	G - T4	0	0	0	0	0	0	6378167.27 ±0.08	6378106.70 ±0.08	6356752.17 ±0.08
	G - T5	-0.11 ±0.13	-0.05 ±0.13	-0.06 ±0.13	0	0	-14.9366733 ±0.0000007	6378171.92 ±0.07	6378102.06 ±0.07	6356752.17 ±0.07
	G - T6	0	0	0	0	0	-14.9366732 ±0.0000007	6378171.92 ±0.07	6378102.06 ±0.07	6356752.17 ±0.07
	T6	0	0	0	0	0	-14.9367	6378171.92	6378102.06	6356752.17
	G - B3	-0.11 ±0.16	-0.05 ±0.16	-0.06 ±0.01	0	0	-	6378136.99 ±0.09		6356752.17 ±0.09
	G - B4	0	0	0	0	0	-	6378136.99 ±0.09		6356752.17 ±0.09
	G - S3	-0.08 ±33	-0.05 ±33	-0.04 ±33	-	-	-	6371037 ±19		
	G - S4	0	0	0	-	-	-	6371037 ±19		

Looking at the differences in the parameter values from the algebraic fitting in the T1 case between the data sets D1.1 and D1.2, one realizes the importance of using a data set of points with uniform surface density (almost equally spaced points). In addition, we also note some minor differences in the values for the Euler angles, which justifies our decision to use the geometric fitting for the study of all subsequent cases and geoid models.

Table 6: Statistics of fitting for the geoid model GOGO06s

Dataset	Fitting – Case	Statistics				
		$a_x - a_y$ (m)	$mean(\hat{N})$ (m)	$min(\hat{N})$ (m)	$max(\hat{N})$ (m)	$rms(\hat{N})$ (m)
D1.1	A - T1	70.13	-0.0002	-74.48	71.73	24.29
D1.2	A - T1	69.854	-0.0002	-71.90	70.30	24.70
	G - T1	69.854	0.000001	-71.89	70.28	24.70
	G - T2	69.86	0.000001	-71.96	70.29	24.70
	G - T3	60.57	0.000001	-78.36	86.29	26.29
	G - T4	60.57	0.000001	-78.43	86.30	26.29
	G - T5	69.86	0.000001	-71.88	70.28	24.70
	G - T6	69.86	0.000001	-71.96	70.29	24.70
	T6	69.86	0.0001	-71.96	70.29	24.70
	G - B3	0	0.000001	-106.24	85.25	30.59
	G - B4	0	0.000001	-106.32	85.33	30.59
	G - S3	0	-0.00006	-14314	7171	6365
	G - S4	0	-0.00006	-14314	7177	6365

From the results presented in Table 6 it is apparent that the translation parameters t_x, t_y and t_z, as well as the rotation angles θ_x and θ_y, have a very small impact to the statistics of the fitting. Therefore, we added the row 'T6' in both Tables 5 and 6, which represent rounded values of the parameters. In addition, we note the agreement of the statistics of the WGS 84 initial data and the statistics of fitting an oblate spheroid (case G - B4 above). In contrast, we note the improvement of the statistics when fitting a triaxial ellipsoid (case G - T6 above). This improvement is visualized in the following Figures 1 to 4. Figures 1 to 3 were created by the free software GMT 6 (Wessel et al. (2019)).

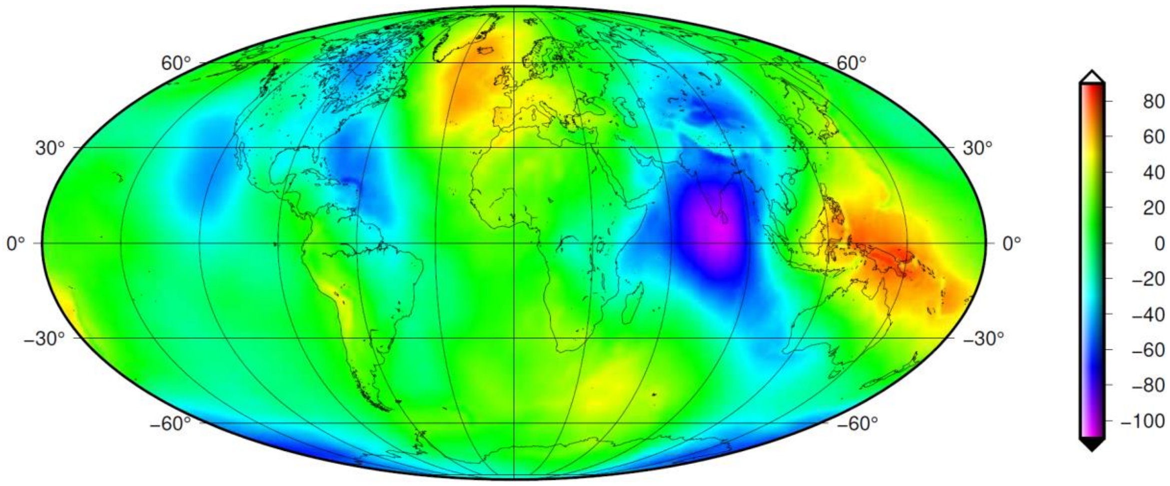

Figure 1: Geoidal heights (in meters) of model GOCO06s with respect to the oblate spheroid WGS 84 in Mollweide projection. $mean = -0.05$ m, $min = -106.33$ m, $max = 85.31$ m, $rms = 30.59$ m.

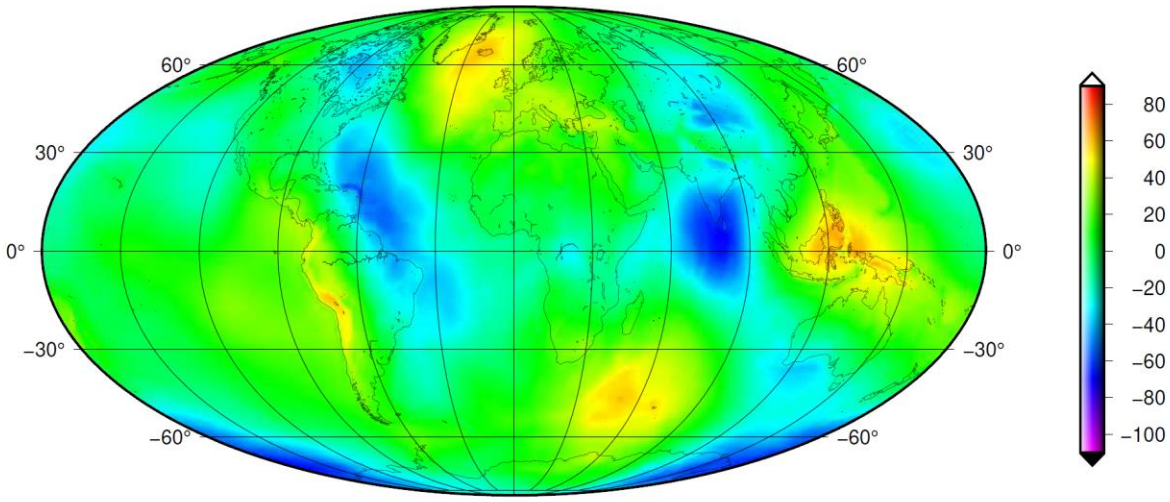

Figure 2: Geoidal heights (in meters) of model GOCO06s with respect to the computed triaxial ellipsoid of case G-T6 in Mollweide projection. $mean = 0.000001$ m, $min = -71.96$ m, $max = 70.29$ m, $rms = 24.70$ m.

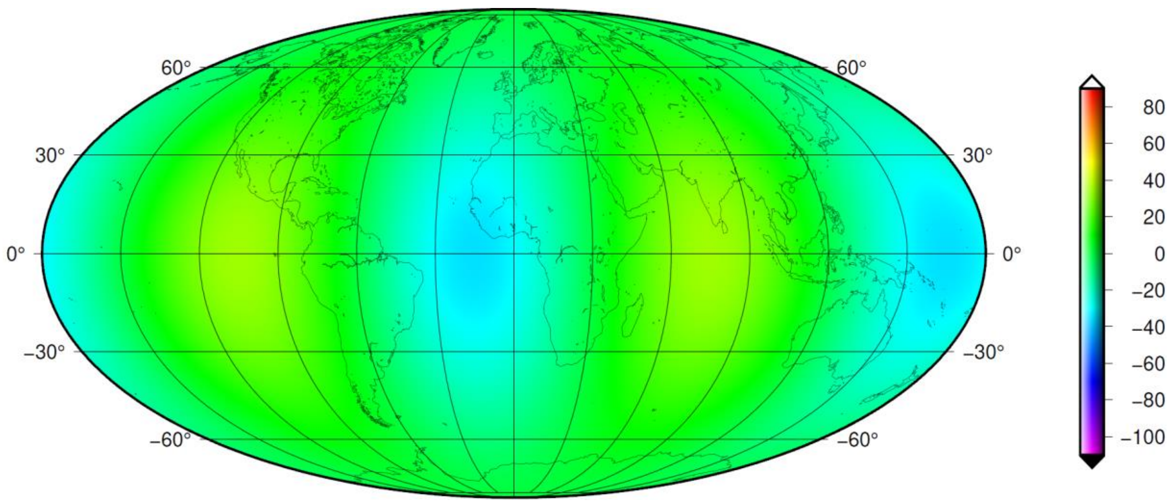

Figure 3: Geoidal heights given in Fig. 2 minus geoidal heights given in Fig. 1 (in meters) in Mollweide projection. $mean = 0.05$ m, $min = -34.92$ m, $max = 34.94$ m.

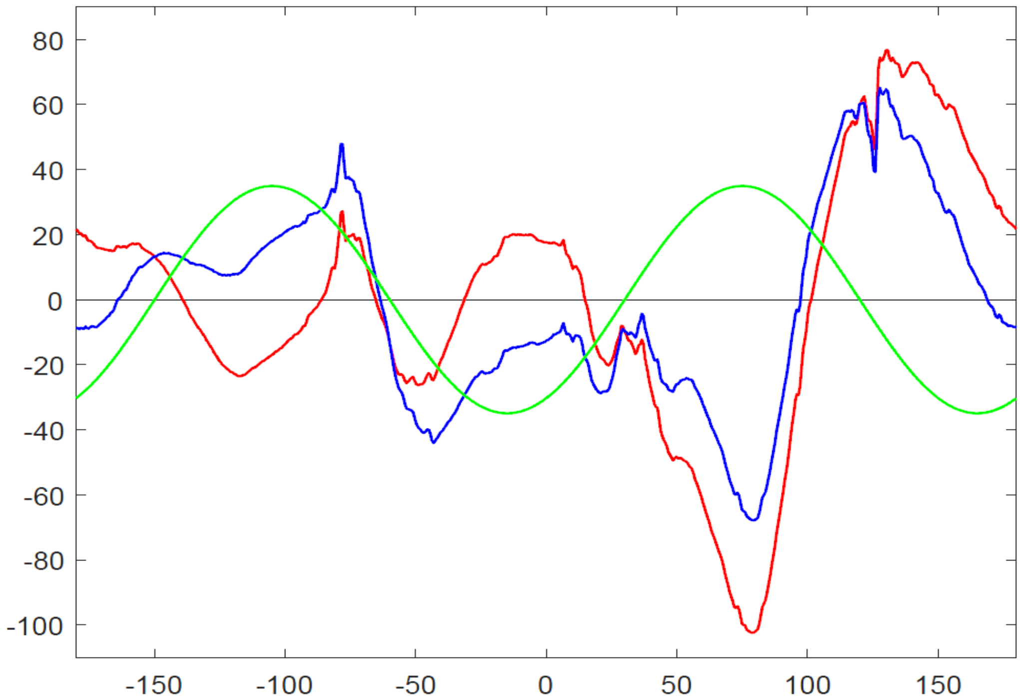

Figure 4: Geoidal heights (in meters – vertical axis) as a cross section along equator (in degrees – horizontal axis) of model GOCO06s with respect to: i) the oblate spheroid WGS 84 (red line) and ii) the computed triaxial ellipsoid of case G-T6 (blue line). The green line illustrates the difference (in meters) in two heights (heights given in blue line minus heights given in red line).

6.3. Results and statistics for the geoid model EGM2008

In order to study the effect of the spatial resolution of the data on the parameters of the fitting, we prepared four different data sets, all based on the geoid model EGM2008, at different resolutions, corresponding to the ones of the other geoid models. The results of the geometric fitting and the relevant statistics (cases G - T6 and G - B4) are presented in Table 7.

Table 7: Resulting values of the parameters and statistics of fitting for the geoid model EGM2008

Dataset	Fitting – Case	Parameters				Statistics				
		θ_z (°)	a_x (m)	a_y (m)	b (m)	$a_x - a_y$ (m)	$mean(\hat{N})$ (m)	$min(\hat{N})$ (m)	$max(\hat{N})$ (m)	$rms(\hat{N})$ (m)
D2.1	G - T6	-14.9356740 ±0.0000005	6378171.88 ±0.06	6378102.03 ±0.06	6356752.24 ±0.06	69.85	0.000001	-71.97	70.49	24.70
	G - B4	-	6378136.96 ±0.08		6356752.24 ±0.08	0	0.00001	-106.38	85.97	30.59
D2.2	G - T6	-14.9369405 ±0.0000005	6378171.90 ±0.07	6378102.04 ±0.07	6356752.20 ±0.07	69.86	0.000001	-71.87	70.45	24.71
	G - B4	-	6378136.97 ±0.09		6356752.20 ±0.09	0	0.000001	-106.23	85.34	30.60
D2.3	G - T6	-14.939350 ±0.000001	6378171.88 ±0.12	6378102.03 ±0.12	6356752.24 ±0.12	69.85	0.000001	-71.46	67.43	24.70
	G - B4	-	6378136.95 ±0.15		6356752.24 ±0.15	0	0.000001	-105.89	85.97	30.60
D2.4	G - T6	-15.12522 ±0.00001	6378172.0 ±1.5	6378102.1 ±1.5	6356751.8 ±1.5	69.9	0.000001	-64.19	60.03	24.75
	G - B4	-	6378137.1 ±1.8		6356751.8 ±1.8	0	0.000001	-94.65	72.33	30.59

From the above values we conclude that the effect of the spatial resolution is insignificant, in the sense that the values are in agreement considering their statistical error bounds.

6.4. Results and statistics for various geoid models

In order to study the performance of different geoid models, going back roughly 50 years ago, we prepared data sets for four geoid models of the past, which were proposed about every 10 years. The results of the geometric fitting and the relevant statistics (cases G - T6 and G - B4) are presented in Table 8.

Table 8: Resulting values of the parameters and statistics of fitting for various geoid models

<table>
<tr><th rowspan="2">Dataset</th><th rowspan="2">Fitting – Case</th><th colspan="4">Parameters</th><th colspan="5">Statistics</th></tr>
<tr><th>θ_z (°)</th><th>a_x (m)</th><th>a_y (m)</th><th>b (m)</th><th>$a_x - a_y$ (m)</th><th>$mean(\hat{N})$ (m)</th><th>$min(\hat{N})$ (m)</th><th>$max(\hat{N})$ (m)</th><th>$rms(\hat{N})$ (m)</th></tr>
<tr><td rowspan="2">D3</td><td>G - T6</td><td>-14.9366367 ±0.0000005</td><td>6378171.88 ±0.06</td><td>6378102.03 ±0.06</td><td>6356752.23 ±0.06</td><td>69.85</td><td>0.000001</td><td>-72.03</td><td>69.85</td><td>24.70</td></tr>
<tr><td>G - B4</td><td>-</td><td colspan="2">6378136.96 ±0.08</td><td>6356752.23 ±0.08</td><td>0</td><td>0.000001</td><td>-106.44</td><td>85.48</td><td>30.59</td></tr>
<tr><td rowspan="2">D4</td><td>G - T6</td><td>-14.9328972 ±0.0000005</td><td>6378171.95 ±0.06</td><td>6378102.13 ±0.06</td><td>6356752.30 ±0.06</td><td>69.82</td><td>0.000001</td><td>-72.90</td><td>66.13</td><td>24.63</td></tr>
<tr><td>G - B4</td><td>-</td><td colspan="2">6378137.04 ±0.08</td><td>6356752.30 ±0.08</td><td>0</td><td>0.000001</td><td>-107.25</td><td>82.16</td><td>30.53</td></tr>
<tr><td rowspan="2">D5</td><td>G - T6</td><td>-14.929005 ±0.000008</td><td>6378171.7 ±0.9</td><td>6378102.0 ±0.9</td><td>6356753.0 ±0.9</td><td>69.7</td><td>0.000001</td><td>-67.88</td><td>68.04</td><td>24.59</td></tr>
<tr><td>G - B4</td><td>-</td><td colspan="2">6378136.9 ±1.1</td><td>6356753.0 ±1.1</td><td>0</td><td>0.000001</td><td>-102.01</td><td>74.55</td><td>30.58</td></tr>
<tr><td rowspan="2">D6</td><td>G - T6</td><td>-14.82805 ±0.00001</td><td>6378215.3 ±1.2</td><td>6378147.4 ±1.2</td><td>6356796.0 ±1.2</td><td>67.9</td><td>0.000001</td><td>-66.82</td><td>58.78</td><td>20.84</td></tr>
<tr><td>G - B4</td><td>-</td><td colspan="2">6378181.4 ±1.6</td><td>6356796.0 ±1.6</td><td>0</td><td>0.000001</td><td>-79.10</td><td>57.23</td><td>27.20</td></tr>
</table>

From the above values we conclude that the estimates for the difference between the equatorial semi-axes, as well as for the longitude of the semi-major axis θ_z, are almost the same.

6.5. Comparison with results from spherical harmonic coefficients

For a near-spherical body, using the spherical harmonic coefficients of degree and order two of a global gravity field model, we can compute the longitude of the principal axis of the least moment of inertia by:

$$\lambda_0 = \frac{1}{2}\tan^{-1}\left(\frac{S_{22}}{C_{22}}\right) \tag{65}$$

and using the reference radius R (which only has the meaning of a scale factor) one gets an expression for the (positive) difference of the two equatorial semi-axes (Liu and Chao (1991))

$$a_x - a_y = R\sqrt{15}\sqrt{C_{22}^2 + S_{22}^2} \tag{66}$$

The uncertainties σ of the above parameters in Eqs. (65) and (66) can be computed by applying the error propagation law:

$$\sigma_{\lambda_0} = \pm \frac{1}{2(C_{22}^2+S_{22}^2)} \sqrt{S_{22}^2 \sigma_{C_{22}}^2 + C_{22}^2 \sigma_{S_{22}}^2} \tag{67}$$

and

$$\sigma_{a_x - a_y} = \pm \frac{R\sqrt{15}}{\sqrt{C_{22}^2+S_{22}^2}} \sqrt{C_{22}^2 \sigma_{C_{22}}^2 + S_{22}^2 \sigma_{S_{22}}^2} \tag{68}$$

where σ_C and σ_S are the uncertainties of the coefficients, as given in a global gravity field model.

Table 9 presents the data and the estimated values for the above parameters for each one of the geoid models used.

Table 9: Data and estimated values for the parameters for the geoid models

Geoid model	R (m)	C_{22}	S_{22}	λ_0 (°)	$a_x - a_y$ (m)
GOGO06s	6378136.3	$2.439370388690 \cdot 10^{-6}$ $\pm 8.092959988764 \cdot 10^{-13}$	$-1.400307620664 \cdot 10^{-6}$ $\pm 9.226405195253 \cdot 10^{-13}$	-14.9288750 ± 0.0000091	69.480959 ± 0.000021
EGM2008	6378136.3	$2.43938357328313 \cdot 10^{-6}$ $\pm 7.230231722 \cdot 10^{-12}$	$-1.40027370385934 \cdot 10^{-6}$ $\pm 7.425816951 \cdot 10^{-12}$	-14.928509 ± 0.000075	69.48082 ± 0.00018
EGM96	6378136.3	$2.43914352398 \cdot 10^{-6}$ $\pm 5.3739154 \cdot 10^{-11}$	$-1.40016683654 \cdot 10^{-6}$ $\pm 5.4353269 \cdot 10^{-11}$	-14.92878 ± 0.00055	69.4744 ± 0.0013
OSU86f	6378136.3	$2.43834012895 \cdot 10^{-6}$	$-1.39928194222 \cdot 10^{-6}$	-14.92504	69.4463
GEM8	6378136.3	$2.4345 \cdot 10^{-6}$	$-1.3953 \cdot 10^{-6}$	-14.90929	69.3151
SE1	6378165	$2.379 \cdot 10^{-6}$	$-1.351 \cdot 10^{-6}$	-14.79581	67.5823

From the estimates in Table 9 we note the high degree of precision of these values, as well as their consistency and the very small difference from the results of the corresponding geometric fitting. Finally, we note that all geoid models do not include the spherical harmonic coefficients of degree one, implying that the translations are assumed zero.

7. Conclusions and future work

In this work, we presented a procedure for the estimation of parameters of Earth's triaxiality through a geometric fitting of a triaxial ellipsoid to a set of given points in space, derived from and representing various geoid models. The condition for the fitting is the minimization of the sum of the squared geoid heights. Taking into consideration the advantages of a satellite-only model (GOCO06s), we conclude that the optimum semi-axes of the triaxial ellipsoid with four parameters are equal to 6378171.92 m, 6378102.06 m and 6356752.17 m, while the longitude of the equatorial major semi-axis is –14.9367 degrees.

The geometric fitting has the added advantage of a straightforward geometric interpretation of the residuals and the a-posteriori variance factor, something that is difficult to achieve with the algebraic fitting.

The geometric fitting presented in this work (with respect to orthogonal distances) is different from the fitting used by Burša (with respect to radial distances). Evidently, the two methods give the same results for a spherical body or quite similar results for a nearly spherical one, like the Earth.

We should note that the procedure to derive the ellipsoidal parameters from the polynomial coefficients (subsection 2.4) is simpler than the corresponding method presented in Bektas (2015). However, it is important to compare the performance of the geometric fitting presented here with the corresponding fitting presented in Bektas (2015).

A further study of the problem of estimating the triaxiality parameters of the Earth could involve other minimization conditions, such as the gravity anomalies (gravimetric method) or the deflections of the vertical.

Using the parameters of the triaxial ellipsoid one could also study the differences between this surface and the adopted oblate spheroid, as well as their effects, not only with respect to the geoid heights but to other geometrical (e.g. geodesic lines) or dynamical characteristics of the Earth.

The procedure presented in this work can also be used for a geometric fitting of the physical surface of the Earth, as mentioned in Tserklevych, Zaiats and Shylo (2016), as well as of the physical surfaces of other celestial bodies, as presented in Karimi, Ardalan and Farahani (2016, 2017), who use an algebraic fitting in their work.

References

Barthelmes F., 2014. Global Models. In: Grafarend E. (Ed.) Encyclopedia of Geodesy, Springer International Publishing. https://doi.org/10.1007/978-3-319-02370-0_43-2

Bektas S., 2015. Least squares fitting of ellipsoid using orthogonal distances. Bol Ciênc Geod 21, 329–339. https://doi.org/10.1590/S1982-21702015000200019

Bektas S., 2014. Orthogonal distance from an ellipsoid. Bol Ciênc Geod 20, 970–983. https://doi.org/10.1590/S1982-21702014000400053

Burša M., 1972. Fundamental geodetic parameters of the earth's figure and the structure of the earth's gravity field derived from satellite data. Stud Geophys Geod 16, 10–29. https://doi.org/10.1007/BF01614229

Burša M., 1971. On the triaxiality of the earth on the basis of satellite data. Stud Geophys Geod 15, 228–240. https://doi.org/10.1007/BF01589239

Burša M., 1970. Best-fitting tri-axial earth ellipsoid parameters derived from satellite observations. Stud Geophys Geod 14, 1–9. https://doi.org/10.1007/BF02585546

Burša M. and Fialová V., 1993. Parameters of the Earth's tri-axial level ellipsoid. Stud Geophys Geod 37, 1–13. https://doi.org/10.1007/BF01613918

Burša M. and Šíma Z., 1980. Tri-axiality of the Earth, the Moon and Mars. Stud Geophys Geod 24, 211–217. https://doi.org/10.1007/BF01634133

Chen W. and Shen W. B., 2010. New estimates of the inertia tensor and rotation of the triaxial nonrigid Earth. J Geophys Res 115, B12419. https://doi.org/10.1029/2009JB007094

Dermanis A., 2017. Fitting Analytical Surfaces to Points: General Approaches and Applications to Ellipsoid Fitting. In: Georgoula O., Papadopoulou M., Rossikopoulos D., Spatalas S., Fotiou A. (Eds.), Living with GIS, In honour of the memory of Professor Ioannis Paraschakis, AUTh, Thessaloniki, Greece, 81–106.

Eitschberger B., 1978. Ein Geodätisches Weltdatum aus Terrestrischen und Satellitendaten. DGK, Reihe C, Heft 245, München.

GMT 6: Wessel P., Luis J. F., Uieda L., Scharroo R., Wobbe F., Smith W. H. F. and Tian D., 2019. The Generic Mapping Tools version 6. Geochemistry, Geophysics, Geosystems, 20, 5556–5564. https://doi.org/10.1029/2019GC008515

Heiskanen W. A., 1962. Is the Earth a triaxial ellipsoid?. J Geophys Res 67, 321–327. https://doi.org/10.1029/JZ067i001p00321

Hirvonen R. A., 1971. Adjustment by least squares in geodesy and photogrammetry. Ungar, New York.

Karimi R., Ardalan A. A. and Farahani S. V., 2017. The size, shape and orientation of the asteroid Vesta based on data from the Dawn mission. Earth and Planetary Science Letters 475, 71–82. https://doi.org/10.1016/j.epsl.2017.07.033

Karimi R., Ardalan A. A. and Farahani S. V., 2016. Reference surfaces of the planet Mercury from MESSENGER. Icarus 264, 239–245. https://doi.org/10.1016/j.icarus.2015.09.035

Kvas A., Mayer-Gürr T., Krauss S., Brockmann J. M., Schubert T., Schuh W.-D., Pail R., Gruber T., Jäggi A. and Meyer U., 2019. The satellite-only gravity field model GOCO06s. GFZ Data Services. http://doi.org/10.5880/ICGEM.2019.002

Ligas M., 2012. Two modified algorithms to transform Cartesian to geodetic coordinates on a triaxial ellipsoid. Stud Geophys Geod 56, 993–1006. https://doi.org/10.1007/s11200-011-9017-5

Liu H. S. and Chao B. F., 1991. The Earth's equatorial principal axes and moments of inertia. Geophysical Journal International 106, 699–702. https://doi.org/10.1111/j.1365-246X.1991.tb06341.x

Lemoine F. G., Kenyon S. C., Factor J. K., Trimmer R. G., Pavlis N. K., Chinn D. S., Cox C. M., Klosko S. M., Luthcke S. B., Torrence M. H., Wang Y. M., Williamson R. G., Pavlis E. C., Rapp R. H. and Olson T. R., 1998. The Development of the Joint NASA GSFC and the National Imagery and Mapping Agency (NIMA) Geopotential Model EGM96. NASA/TP-1998-206861, NASA Goddard Space Flight Center, Greenbelt, Maryland.

Lundquist C. A. and Veis G., 1966. Geodetic Parameters for a 1966 Smithsonian Institution Standard Earth. Smithsonian Astrophysical Observatory, Special Report No. 200, Cambridge, Massachusetts.

Mikhail E. M., (with contributions by Ackermann F.), 1976. Observations and least squares. IEP – A Dun – Donnelley Publisher, New York.

NIMA, 2000. Department of Defense World Geodetic System 1984 (3rd), US National Imagery and Mapping Agency, Technical Report, 8350.2.

Pavlis N. K., Holmes S. A., Kenyon S. C. and Factor J. K., 2012. The development and evaluation of the Earth Gravitational Model 2008 (EGM2008). J Geophys Res 117, B04406. https://doi.org/10.1029/2011JB008916

Panou G. and Korakitis R., 2019. Cartesian to geodetic coordinates conversion on a triaxial ellipsoid using the bisection method. Preprint, https://www.researchgate.net/publication/333904072_Cartesian_to_geodetic_coordinates_conversion_on_a_triaxial_ellipsoid_using_the_bisection_method

Rapp R. H. and Cruz J. Y., 1986. Spherical Harmonic Expansions of the Earth's Gravitational Potential to Degree 360 Using 30' Mean Anomalies. The Ohio State University, Department of Geodetic Science and Surveying, Report No. 376, Columbus, Ohio.

Tserklevych A. L., Zaiats O. S. and Shylo Y., 2016. Approximation of the physical surface of the Earth by biaxial and triaxial ellipsoid. Geodynamics 20, 40–49.

Wagner C. A., Lerch F. J., Brownd J. E. and Richardson J. A., 1977. Improvement in the geopotential derived from satellite and surface data (GEM 7 and 8). J Geophys Res 82, 901–914. https://doi.org/10.1029/JB082i005p00901